PERFORMANCE OF SPATIAL MULTIPLEXING IN THE PRESENCE OF POLARIZATION DIVERSITY

Helmut Bölcskei[1)], *Rohit U. Nabar*[1)], *V. Erceg*[2)], *D. Gesbert*[2)], *and Arogyaswami J. Paulraj*[1)]

[1)] Information Systems Laboratory, Stanford University
Packard 223, 350 Serra Mall, Stanford, CA 94305-9510
Phone: (650)-724-3640, Fax: (650)-723-8473, email: bolcskei@stanford.edu
[2)] Iospan (formerly Gigabit) Wireless Inc., 3099 North First Street, San Jose, CA 95134

Abstract—In practice large antenna spacings are needed to achieve high capacity gains in multiple-input multiple-output (MIMO) wireless systems. The use of dual-polarized antennas is a promising cost effective alternative where two spatially separated antennas can be replaced by a single antenna element employing orthogonal polarizations. This paper investigates the performance of *spatial multiplexing* in MIMO wireless systems with dual-polarized antennas. We compute estimates of the symbol error rate as a function of cross-polarization discrimination (XPD) and spatial fading correlations. Using these estimates, we show that dual-polarized antennas can significantly improve the performance of spatial multiplexing systems. It is demonstrated that improvements in terms of symbol error rate of up to an order of magnitude are possible. We furthermore find that in general for a given SNR there is an optimum XPD for which the symbol error rate is minimum. Finally, we present simulation results and we show that our estimates closely match the numerical results.

1. INTRODUCTION AND OUTLINE

The use of multiple antennas at both ends of a wireless link has recently been shown to have the potential of drastically increasing capacity through a technique called *spatial multiplexing* [1]-[5]. This capacity gain depends strongly on transmit and receive antenna spacing. In practice antenna spacings of several wavelengths are required in order to achieve significant multiplexing gain. Unfortunately, large antenna spacing increases both size and cost of base stations and renders the use of multiple antennas in handsets very difficult. The use of dual-polarized antennas is a promising cost effective alternative where two spatially separated antennas can be replaced by a single antenna element employing orthogonal polarizations.

Contributions. In this paper, we investigate the performance of uncoded spatial multiplexing in systems employing dual-polarized antennas. Although our techniques are generally applicable, for the sake of simplicity, we consider a link with one dual-polarized transmit and one dual-polarized receive antenna. Our contributions are as follows.

- We introduce a *channel model* for a dual-polarized single-input single-output link taking into account spatial fading correlations and cross-polarization discrimination (XPD).
- We propose a method for *computing estimates of the uncoded symbol error rate* of spatial multiplexing in the presence of polarization diversity.
- We *identify the propagation conditions* where the use of *polarization diversity is beneficial* from an error-probability point of view, and we show that improvements in terms of symbol error rate of up to an order of magnitude are possible.
- We demonstrate that our *symbol error estimates closely match the simulation results*. Our method can therefore be used to *predict performance trends* analytically and helps avoiding time-consuming computer simulations.

Organization of the paper. The rest of this paper is organized as follows. Section 2 introduces the channel model for a dual-polarized single-input single-output link and states our assumptions. In Section 3, we derive estimates for the uncoded symbol error rate of spatial multiplexing as a function of spatial fading correlations, XPD, and SNR. Section 4 provides simulation results and demonstrates that our estimates closely match the simulation results. Finally, Section 5 contains our conclusions.

2. THE CHANNEL MODEL

We consider a system with one dual-polarized transmit and one dual-polarized receive antenna. The channel is assumed to be flat over the frequency-band of interest. The input-output relation is therefore given by[1]

$$\mathbf{r} = \sqrt{E_s}\,\mathbf{H}\,\mathbf{x} + \mathbf{n}, \tag{1}$$

where $\mathbf{x} = [x_0 \; x_1]^T$ is the 2×1 transmit signal vector whose elements are taken from a finite (complex) constellation chosen such that the average energy of the constellation elements is 1, $\mathbf{r} = [r_0 \; r_1]^T$ is the 2×1 receive signal vector, $\mathbf{n}$ is complex-valued gaussian noise with $\mathcal{E}\{\mathbf{n}\mathbf{n}^H\} = \sigma_n^2 \mathbf{I}_2$,

$$\mathbf{H} = \begin{bmatrix} h_{0,0} & h_{0,1} \\ h_{1,0} & h_{1,1} \end{bmatrix}$$

The work of H. Bölcskei was supported by FWF grant J1868-TEC. R. Nabar's work was supported by the Dr. T. J. Rodgers Stanford Graduate Fellowship. H. Bölcskei is on leave from the Institut für Nachrichtentechnik und Hochfrequenztechnik, Technische Universität Wien, Vienna, Austria.

[1]The superscripts ^{T} and ^{H} stand for transpose and conjugate transpose, respectively.

0-7803-7041-4/01/$10.00 ©2001 IEEE

Authorized licensed use limited to: ETH BIBLIOTHEK ZURICH. Downloaded on January 30, 2010 at 04:09 from IEEE Xplore. Restrictions apply.

is the channel transfer matrix which is also the polarization matrix, and $\sqrt{E_s}$ is a normalization factor. The polarization matrix describes the degree of suppression of individual co- and cross-polarized components, cross correlation, and cross coupling of energy from one polarization state to the other polarization state. In practice, the following polarizations are generally considered: *horizontol, vertical, and* $\pm 45^\circ$ *slanted* polarization. In this paper, we assume that the transmitter and the receiver employ the same polarizations, i.e., both of them employ horizontal and vertical polarization for example. The signals x_0 and x_1 are transmitted on the two different polarizations, and r_0 and r_1 are the signals received on the corresponding polarizations. We emphasize that although we are dealing with one physical transmit and one physical receive antenna, the underlying channel is a 2−input 2−output channel, since each polarization mode is treated as an independent physical channel. We assume that the channel is purely Rayleigh fading, i.e., the matrix $\mathbf{H}$ consists of (in general correlated) complex gaussian random variables with zero mean. The more general case taking into account a line-of-sight component is treated in [6]. The correlation between the elements of the matrix $\mathbf{H}$ and the variances of the elements depend on the propagation conditions and the choice of polarizations, respectively.

Throughout the paper, we assume[2]

$$\mathcal{E}\{|h_{0,0}|^2\} = \mathcal{E}\{|h_{1,1}|^2\} = 1$$
$$\mathcal{E}\{|h_{0,1}|^2\} = \mathcal{E}\{|h_{1,0}|^2\} = \alpha,$$

where $0 < \alpha \leq 1$ depends on the XPD. Good XPD yields small α and vice versa. The case $\alpha = 1$ can also be interpreted as having two physical antennas on each side of the link employing the same polarization. We furthermore define the following correlation coefficients[3]

$$t = \frac{\mathcal{E}\{h_{0,0}h_{0,1}^*\}}{\sqrt{\alpha}} = \frac{\mathcal{E}\{h_{1,0}h_{1,1}^*\}}{\sqrt{\alpha}}$$
$$r = \frac{\mathcal{E}\{h_{0,0}h_{1,0}^*\}}{\sqrt{\alpha}} = \frac{\mathcal{E}\{h_{0,1}h_{1,1}^*\}}{\sqrt{\alpha}}.$$

For the sake of simplicity, throughout the paper, we assume that $\mathcal{E}\{h_{0,0}h_{1,1}^*\} = \mathcal{E}\{h_{1,0}h_{0,1}^*\} = 0$. Measured values of XPD and correlation coefficients have been reported for example in [7]-[9].

3. DERIVATION OF SYMBOL ERROR RATE

In this section, we first discuss the impact of polarization diversity on spatial multiplexing and then compute an estimate of the symbol error rate.

3.1. Impact of Polarization Diversity

Spatial multiplexing [1]-[5] has the potential to dramatically increase the capacity of wireless radio links with no additional power or bandwidth consumption. The basic idea is that if scattering in the multi-antenna channel is rich enough independent parallel spatial data pipes are created within the same bandwidth, which ideally yields a linear (in the number of antennas) capacity increase. Traditionally, the ability to perform spatial multiplexing has been related to a rich enough scattering environment. In the present case virtual multiple antennas are created by employing different polarizations and the MIMO channel matrix is replaced by the polarization matrix. It is therefore not clear a priori how spatial multiplexing will perform in the presence of polarization diversity and how the exact values of XPD and fading correlations will influence the performance. We can, however, quantitatively establish the benefit of polarization diversity. It is well known that the multiplexing gain is maximized if the condition number of the channel matrix is 1. Now, it is intuitively clear that for small α the individual realizations of $\mathbf{H}$ tend to have lower condition number. In fact, in the limiting case $\alpha = 0$ (i.e. perfect XPD) every realization of $\mathbf{H}$ yields orthogonal columns and hence high multiplexing gain can be expected.

3.2. Error Probability

Throughout the paper, we assume that the channel is unknown in the transmitter, perfectly known in the receiver, and that maximum-likelihood (ML) decoding is performed. The receiver computes the ML estimate according to

$$\hat{\mathbf{x}} = \arg\min_{\mathbf{x}} \|\mathbf{r} - \sqrt{E_s}\mathbf{H}\mathbf{x}\|^2,$$

where the minimization is performed over the set of all possible codevectors.

Let $\mathbf{c}$ and $\mathbf{e}$ be two different codevectors of size 2×1 and assume that $\mathbf{c}$ was transmitted. For a given channel realization $\mathbf{H}$, the probability that the receiver decides erroneously in favor of the vector $\mathbf{e}$ is given by [10]

$$P(\mathbf{c} \to \mathbf{e}|\mathbf{H}) = Q\left(\sqrt{\frac{E_s}{2\sigma_n^2} d^2(\mathbf{c}, \mathbf{e}|\mathbf{H})}\right), \qquad (2)$$

where

$$d^2(\mathbf{c}, \mathbf{e}|\mathbf{H}) = \|\mathbf{H}(\mathbf{c} - \mathbf{e})\|^2.$$

Upon defining $\mathbf{y} = \mathbf{H}(\mathbf{c} - \mathbf{e})$ we get $d^2(\mathbf{c}, \mathbf{e}|\mathbf{H}) = \|\mathbf{y}\|^2$ and hence using the Chernoff bound $Q(x) \leq e^{-x^2/2}$ it follows from (2) that

$$P(\mathbf{c} \to \mathbf{e}|\mathbf{H}) \leq e^{-\frac{E_s}{4\sigma_n^2}\|\mathbf{y}\|^2}. \qquad (3)$$

Since $\mathbf{H}$ was assumed to be gaussian it follows that the 2×1 vector $\mathbf{y}$ is gaussian as well. The average over all channel realizations of the right-hand side in (3) is fully characterized by the eigenvalues of the 2×2 covariance matrix of $\mathbf{y}$ [11] defined as $\mathbf{C}_y = \mathcal{E}\{\mathbf{y}\mathbf{y}^H\}$. In particular, denoting the eigenvalues of $\mathbf{C}_y$ as $\lambda_i(\mathbf{C}_y)$, we get

$$P(\mathbf{c} \to \mathbf{e}) \leq \frac{1}{1 + \lambda_1(\mathbf{C}_y)\frac{E_s}{4\sigma_n^2}} \frac{1}{1 + \lambda_2(\mathbf{C}_y)\frac{E_s}{4\sigma_n^2}}, \qquad (4)$$

where $P(\mathbf{c} \to \mathbf{e}) = \mathcal{E}_H\{P(\mathbf{c} \to \mathbf{e}|\mathbf{H})\}$ is the pairwise error probability averaged over all channel realizations. Straightforward manipulations reveal that[4] $\mathbf{C}_y =$

$$\begin{bmatrix} |c_0 - e_0|^2 + \alpha|c_1 - e_1|^2 + 2\mathcal{R}\{(c_0 - e_0)(c_1 - e_1)^* t\sqrt{\alpha}\} & r^*\sqrt{\alpha}(|c_0 - e_0|^2 + |c_1 - e_1|^2) \\ r\sqrt{\alpha}(|c_0 - e_0|^2 + |c_1 - e_1|^2) & \alpha|c_0 - e_0|^2 + |c_1 - e_1|^2 + 2\mathcal{R}\{(c_0 - e_0)(c_1 - e_1)^* t\sqrt{\alpha}\} \end{bmatrix}.$$

The eigenvalues of $\mathbf{C}_y$ are given by

[2] $\mathcal{E}$ stands for the expectation operator.

[3] The superscript * stands for complex conjugate.

[4] $\mathcal{R}\{a\}$ stands for the real part of a.

Authorized licensed use limited to: ETH BIBLIOTHEK ZURICH. Downloaded on January 30, 2010 at 04:09 from IEEE Xplore. Restrictions apply.

$$\lambda_{1,2} = \frac{a + d \pm \sqrt{(a-d)^2 + 4bc}}{2}$$

with

$$\begin{aligned} a &= |c_0 - e_0|^2 + \alpha|c_1 - e_1|^2 \\ &+ 2\mathcal{R}\{(c_0 - e_0)(c_1 - e_1)^* t\sqrt{\alpha}\} \\ b &= r\sqrt{\alpha}(|c_0 - e_0|^2 + |c_1 - e_1|^2) \\ c &= r^*\sqrt{\alpha}(|c_0 - e_0|^2 + |c_1 - e_1|^2) \\ d &= \alpha|c_0 - e_0|^2 + |c_1 - e_1|^2 \\ &+ 2\mathcal{R}\{(c_0 - e_0)(c_1 - e_1)^* t\sqrt{\alpha}\}. \end{aligned}$$

If no polarization diversity is used (i.e. $\alpha = 1$) and the channel matrix is i.i.d., we have $\lambda_1 = \lambda_2 = (|c_0 - e_0|^2 + |c_1 - e_1|^2)$. In this case the error rate behavior is governed by error events where only one out of the two symbols is in error, say $(c_0 - e_0) \neq 0$ with $|c_0 - e_0|^2 = d_{min}^2$ where d_{min} denotes the minimum distance of the scalar constellation used. Clearly, the error rate will decay for increasing d_{min}. In the general case, where $\alpha < 1$ and the individual entries in $\mathbf{H}$ are correlated the error events governing the performance of spatial multiplexing depend on the channel geometry induced by the correlation coefficients and the value of α. In order to avoid having to find those error events for a particular channel geometry, we average over all possible error events including a weighting which takes into account that different vector error events cause a different number of scalar symbol error events. In particular, we want to study the influence of XPD on the error rate of spatial multiplexing systems. It is therefore crucial to reveal how the error probability behaves as a function of XPD for a given SNR and given t and r. We assume that 4-PSK is employed. This implies that there are 240 error events. The individual scalar error events $(c_i - e_i)$ can take values from the set $\{0, \pm d_{min}, \pm j d_{min}, \pm d_{min}(1+j), \pm d_{min}(1-j)\}$. Now, with the relative frequency of an error event ϵ_i where $\mathbf{c}_i - \mathbf{e}_i = [(c_{0,i} - e_{0,i})\ (c_{1,i} - e_{1,i})]^T$ given by

$$n_{\epsilon_i} = \frac{\omega(c_{0,i} - e_{0,i})\,\omega(c_{1,i} - e_{1,i})}{240}$$

with

$$\omega(x) = \begin{cases} 4, & x = 0 \\ 2, & x = \pm d_{min}, \pm j d_{min} \\ 1, & \pm d_{min}(1+j), \pm d_{min}(1-j) \end{cases},$$

we estimate the average symbol error rate as

$$\bar{P} = \sum_{\epsilon_i} n_{\epsilon_i} P(\epsilon_i) s(\epsilon_i). \qquad (5)$$

Here, $P(\epsilon_i)$ is (4) evaluated for $[(c_{0,i} - e_{0,i})\ (c_{1,i} - e_{1,i})]^T$ and

$$s(\epsilon_i) = \begin{cases} 2, & (c_{0,i} - e_{0,i}) \neq 0,\ (c_{1,i} - e_{1,i}) \neq 0 \\ 1, & (c_{0,i} - e_{0,i}) = 0 \quad \text{or} \quad (c_{1,i} - e_{1,i}) = 0. \end{cases}$$

In the next section, $\bar{P}$ is shown to reveal all the relevant trends and a close match between the exact symbol error rate and $\bar{P}$ is found.

We note that (4) can be used to study the impact of t, r and α on $\bar{P}$ analytically. For example, it follows immediately from (4) and (5) that for $t = r = 0$ the quantity $\bar{P}$ will be minimum for $\alpha = 1$, i.e., for the case where no polarization diversity is employed. Indeed, we will find in the next section that polarization diversity improves the multiplexing gain *only* in the presence of high correlations.

4. SIMULATION RESULTS

In this section, we provide simulation results demonstrating the performance of spatial multiplexing in the presence of polarization diversity and spatial fading correlation. In particular, we show that $\bar{P}$ reveals the impact of polarization diversity on the performance of spatial multiplexing quite accurately. We simulated a system with 1 dual-polarized transmit and 1 dual-polarized receive antenna using 4-PSK and employing an ML receiver. The signal-to-noise-ratio (SNR) was defined as $\text{SNR} = 10 \log\left(\frac{2E_s}{\sigma_n^2}\right)$.

Simulation Example 1. The first simulation example serves to demonstrate that $\bar{P}$ provides an accurate estimate of the symbol error rate for high SNR. For $t = 0.5, r = 0.3$ and $\alpha = 0.4$, Fig. 1 shows the symbol error rate obtained using Monte Carlo simulations along with the estimated symbol error rate $\bar{P}$. It can be seen that especially in the high SNR regime the two curves match well. Note, however, that $\bar{P}$ is not a strict upper bound on the symbol error rate.

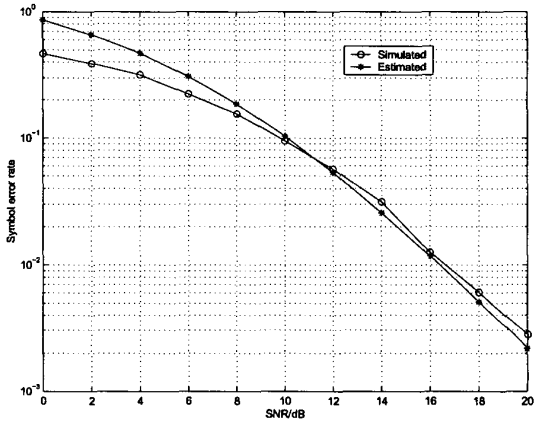

Fig. 1. Symbol error rate as a function of SNR.

Simulation Example 2. The second simulation example serves to demonstrate the benefit of polarization diversity. For an SNR of 15dB, Fig. 2 shows the symbol error rate along with $\bar{P}$ as a function of α for various values of t and for $r = 0$. It can be seen that for low transmit correlation the use of polarization diversity leads to a performance degradation or equivalently reduced multiplexing gain. (Recall that $\alpha = 1$ can be interpreted as having two physical antennas on each side of the link all of which employ the same polarization.) This result conforms with the investigations in the last paragraph of Sec. 3.2. When the transmit correlation starts to increase and the condition number of the channel matrix realizations increases or equivalently the angle between the realizations of the two columns decreases, polarization diversity yields improved spatial separation and hence increases the multiplexing gain. We found that starting at $t = 0.85$ polarization diversity, i.e., $\alpha < 1$ starts improving the multiplexing gain. We can also see that in the case of fully correlated transmit antennas, i.e., $t = 1$, there is an optimum value of α for which the symbol error rate is minimum. Observe that this minimum is accurately predicted by $\bar{P}$. Fig. 2 furthermore shows that for high transmit correlation the use of polarization diversity can improve the symbol error rate by up

Authorized licensed use limited to: ETH BIBLIOTHEK ZURICH. Downloaded on January 30, 2010 at 04:09 from IEEE Xplore. Restrictions apply.

to an order of magnitude.

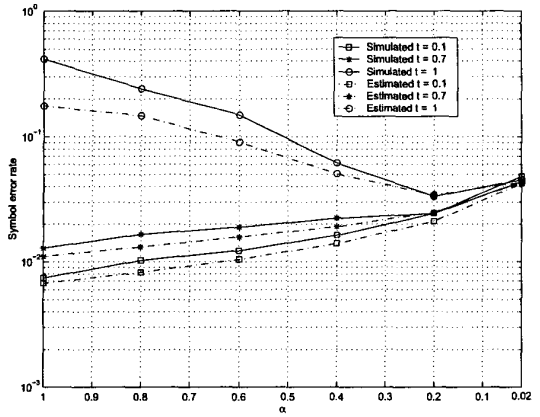

Fig. 2. Symbol error rate as a function of α for various values of the transmit correlation coefficient t.

Simulation Example 3. In the last simulation example, we study the performance of spatial multiplexing with and without polarization diversity in the presence of receive correlation only. Fig. 3 shows the symbol error rate along with $\bar{P}$ for $t = 0$ and various values of r. We observe that for $r = 1$ the use of polarization diversity increases the multiplexing gain or equivalently reduces the symbol error rate. This effect, however, is much less pronounced than in the case of transmit correlation only. The reason for this is that in the presence of transmit correlation there are code vectors which "tend to excite the null space of the channel matrix" and hence yield very high probability of error. This does not happen in the case of receive correlation only. A more detailed description of this observation is provided in [12]. For $r = 1$, the optimum value of α seems to be the same as in the case of transmit correlation only with $t = 1$.

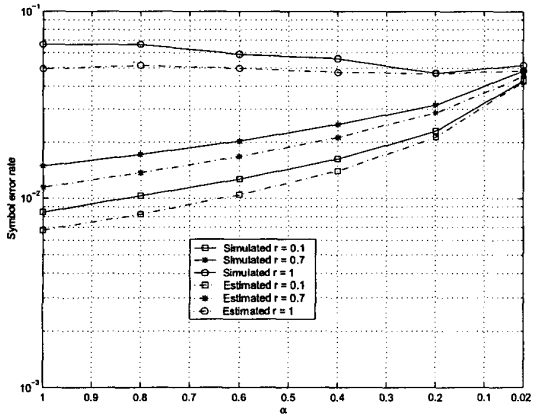

Fig. 3. Symbol error rate as a function of α for various values of the receive correlation coefficient r.

5. CONCLUSION

We studied the use of polarization diversity for spatial multiplexing and found that in the presence of high spatial fading correlation *dual-polarized antennas* can yield a *significantly improved multiplexing gain*. In particular, we computed an estimate of the uncoded symbol error rate which was found to be very accurate in the high SNR regime and which allows to study the impact of polarization diversity on the performance of spatial multiplexing without having to resort to time-consuming computer simulations. We demonstrated that especially in the presence of transmit correlation the use of polarization diversity can yield significant improvements in terms of symbol error rate. Furthermore, we found that for high spatial fading correlation and for a given SNR in general there is an optimum value of α for which the symbol error rate is minimum. Our symbol error estimate accurately predicts this point. Finally, we provided simulation results.

6. REFERENCES

[1] A. J. Paulraj and T. Kailath, "Increasing capacity in wireless broadcast systems using distributed transmission/directional reception," *U. S. Patent*, no. 5,345,599, 1994.

[2] G. J. Foschini, "Layered space-time architecture for wireless communication in a fading environment when using multi-element antennas," *Bell Labs Tech. J.*, pp. 41–59, Autumn 1996.

[3] I. E. Telatar, "Capacity of multi-antenna gaussian channels," Tech. Rep. #BL0112170-950615-07TM, AT & T Bell Laboratories, 1995.

[4] G. G. Raleigh and J. M. Cioffi, "Spatio-temporal coding for wireless communication," *IEEE Trans. Comm.*, vol. 46, no. 3, pp. 357–366, 1998.

[5] H. Bölcskei, D. Gesbert, and A. J. Paulraj, "On the capacity of OFDM-based spatial multiplexing systems," *IEEE Trans. Comm.*, Oct. 1999. submitted.

[6] H. Bölcskei, R. U. Nabar, V. Erceg, D. Gesbert, and A. J. Paulraj, "Performance of multi-antenna signaling strategies in the presence of polarization diversity," *IEEE J. Sel. Areas Comm.*, 2000. to be submitted.

[7] T. Neubauer and P. C. F. Eggers, "Simultaneous characterization of polarization matrix components in pico cells," in *IEEE VTC - Fall*, vol. 3, (Amsterdam (The Netherlands)), pp. 1361 – 1365, 1999.

[8] J. J. A. Lempiäinen and J. K. Laiho-Steffens, "The performance of polarization diversity schemes at a base station in small/micro cells at 1800 MHz," *IEEE Trans. Veh. Tech.*, vol. 47, pp. 1087 – 1092, Aug. 1999.

[9] R. G. Vaughan, "Polarization diversity in mobile communications," *IEEE Trans. Veh. Tech.*, vol. 39, pp. 177 – 186, Aug. 1990.

[10] J. G. Proakis, *Digital Communications*. New York: McGraw-Hill, 3rd ed., 1995.

[11] G. L. Turin, "The characteristic function of hermitian quadratic forms in complex normal variables," *Biometrika*, vol. 47, pp. 199–201, 1960.

[12] H. Bölcskei and A. J. Paulraj, "Performance of space-time codes in the presence of spatial fading correlation," in *Asilomar Conf. on Signals, Systems, and Computers*, (Pacific Grove, CA), Oct. 2000.

Authorized licensed use limited to: ETH BIBLIOTHEK ZURICH. Downloaded on January 30, 2010 at 04:09 from IEEE Xplore. Restrictions apply.